Cu/Co-salen immobilized MCM-41: characterization and catalytic reactions

P. Karandikar, K.C. Dhanya, S. Deshpande, A.J. Chandwadkar,
S. Sivasanker, M. Agashe *

Catalysis Division, National Chemical Laboratory, Pune 411008, India

Abstract

Copper and cobalt (salen) complexes immobilized on the walls of MCM-41 modified with aminopropyl groups have been synthesized and characterized by various physico-chemical measurements such as XRD, FTIR, UV–Vis, EPR, TGA. UV–Vis and FTIR spectra reveal adduct formation of metal–salen complexes with the amino groups tethered to the SiO_2 surface. EPR studies indicate molecular dispersion of the salen complex inside the pores of MCM-41. The activity of the immobilized complexes as catalyst for the liquid phase oxidation of olefins was investigated.
© 2003 Elsevier B.V. All rights reserved.

Keywords: Co/Cu-salen; NH_2–MCM-41; Adduct formation; M–S–AM(PS); Epoxidation

1. Introduction

The development of environment friendly technologies has promoted much research in heterogeneous catalysis and in particular the heterogenization of known active homogeneous catalysts for oxidation [1]. Several model complexes containing porphyrin and schiff base ligands have been synthesized and studied for their oxygen uptake and oxidative catalysis [2–4]. Flexibility of the ethylenediamine backbone in salen as observed in a number of transition metal complexes with bidentate oxygen ligands [5] is responsible for the complex to mimic the biological activity of enzymes.

It has been observed that in addition to catalase activity, metal salens also catalyze a peroxidative reaction between H_2O_2 and oxidizable substrates [6]. One of the major drawbacks of using metal salens in homogenous solutions is the formation of μ-oxo dimers and other polymeric species which leads to irreversible catalyst deactivation. The problem has been avoided in principle by isolating the metal–salen complexes from each other by encapsulation in the cavities of molecular sieves. In recent years, encapsulation of salen complexes in porous materials, typically zeolites, has been extensively studied in an attempt to prepare isolated catalytically active centers that do not undergo rapid degradation as the homologous analogous [7–9].

In the present work, details of preparation and characterization of MCM-41 with isolated covalently bonded metal (salen) complexes are presented.

2. Experimental

2.1. General

MCM-41 was synthesized according to the published procedures [10,11]. The molar composition of the synthesis gel in terms of oxides was as follows:

$$SiO_2 : 0.086\ (NH_4)_2O : 0.089\ (CTMA)_2O$$
$$: 0.155\ (TMA)_2O : 40\ H_2O.$$
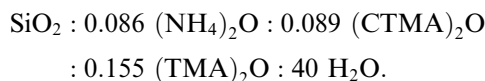
The crystalline phase identification and purity of the as synthesized, calcined and modified samples was carried

---

out by XRD (Rigaku; Miniflex) using a Nickel filtered Cu Kα radiation ($\lambda = 1.5406$ Å). The solid state magic-angle spinning (MAS) NMR studies were carried out on a Bruker MSL-500 FT-NMR spectrometer. The FTIR spectra in the mid-IR region were recorded on KBr pellets using a Shimadzu FT-IR spectrometer (Model 8300). The UV–Vis spectra were recorded using a nujol mull on a SHIMADZU, UV-2101 PC spectrometer. EPR spectra were recorded on a Bruker EMX, X band spectrometer (microwave frequency 9.45 GHz) with 100 kHz-field modulation. Measurements were performed on powder samples at 298 and 77 K. The surface area and pore volume were determined from N_2 adsorption isotherm using a NOVA1200 (Quantachrome) instrument. The samples were degassed at 150 °C for 4 h at 10^{-5} Torr prior to surface area measurement. Thermogravimetric analyses (TGA) were performed on a TG 50 (Mettler) analyzer. All the products of the catalytic reactions were quantified at different intervals by a gas chromatograph (Hewlett-Packard 5880) equipped with a carbo-wax column. The identity of the product was further confirmed by GC-IR (Perkin–Elmer GC-IR 2000 system).

2.2. Ligand preparation

The Schiff's base ligand salen was prepared and purified according to the established procedures [12]. The metal–salen complexes were synthesized under inert condition. An equimolar amount of an ethanolic solution of $M(OAc)_2 \cdot 4H_2O$ (0.03 M) was mixed with the schiff base ligand (0.03 M in ethanol). The mixture was then refluxed for 4 h under N_2 atmosphere. The solid product was filtered, washed with cold ethanol, dried under vacuum and recrystallized in chloroform to get Cu and Co(salen). The purity of the complexes was determined by elemental analysis and FT-IR spectroscopy.

2.3. Catalyst preparation

A solution of 0.240 g of Cu(salen) [0.236 g for Co(salen)] in 20 ml of toluene was stirred and slowly added to a suspension of 0.5 g of NH_2–MCM-41 in toluene [13]. It was stirred over night. A green material was [brown material for Co(salen)] separated by filtration, washed with acetone, dried at ambient temperature and designated as Cu(salen)–NH_2–MCM-41(PS) or Cu–S–AM(PS) [Co–S–AM(PS) for Co(salen) NH_2–MCM-41]. The metal loading was found to be about 4% for both the metals as determined from AAS.

The above procedure was followed with silica gel for the immobilization of the salen complexes. The corresponding complexes are designated as Cu–S–$ASiO_2$ and Co–S–$ASiO_2$.

2.4. Catalytic experiments

Catalytic reactions were carried out at 60 °C in a round bottomed flask fitted with a condenser. All the olefins (99% pure), acetonitrile (99% pure) and TBHP in decane (5.5 M) were used without further purification. Olefins (5 mmol), TBHP as oxidant (5 mmol), acetonitrile as a solvent (10 g) and catalyst (0.05 g) along with toluene as the internal standard were introduced into a round bottom flask. The reactions were carried out with vigorous stirring.

3. Results and discussion

3.1. X-ray diffraction

The XRD patterns of the as synthesized, calcined, and modified MCM-41 samples were compared. The spectra of calcined HSi–MCM-41 showed a marginal decrease in "d" value due to the removal of the template on calcination. The XRD pattern of samples Cu–S–AM(PS) and Co–S–AM(PS), prepared by post-synthesis method, is similar to the parent HSi–MCM-41.

3.2. Solid state MAS NMR spectroscopy

The reaction of 3-APTES with the –OH groups on the walls of HSi–MCM-41 is revealed by the decrease of the silanol signals Q_2 (−91.6 ppm) and Q_3 (−101.15 ppm) and the appearance of a signal characteristic of $(SiO)_3Si$–CH_3 group (−68.22 ppm) in the ^{29}Si MAS NMR spectrum. CP MAS NMR of NH_2–MCM-41 shows aminopropyl carbon signals at 6.4, 18.1 and 39.2 ppm (spectra not presented) [14].

3.3. IR spectroscopy

The IR spectra (recorded using fluorolube mull) of Cu(salen), Cu–S–AM(PS) and Cu(salen)–hexylamine in the 4000–1300 cm^{-1} range are presented in Fig. 1. The bands at 2974 and 2929 cm^{-1} are assigned to the stretching mode of –CH_2 groups. From the presence of these bands it can be inferred that the wall of MCM-41 is modified by aminopropyl groups successfully after the reaction between 3-APTES and the silanol groups in MCM-41. The presence of Cu(salen) is clearly noticeable in the IR spectrum of Cu–S–AM(PS). This supports the incorporation of Cu(salen) in MCM-41. The absorption due to the amino group is not observed in the spectrum of Cu–S–AM(PS), instead a broad band centered at ∼3300 cm^{-1} is observed [13]. In order to study the origin of this band, the spectrum of Cu(salen)–hexylamine adduct was compared. Both the spectra show the broad band centered around 3300 cm^{-1} without any significant change in the bands of salen
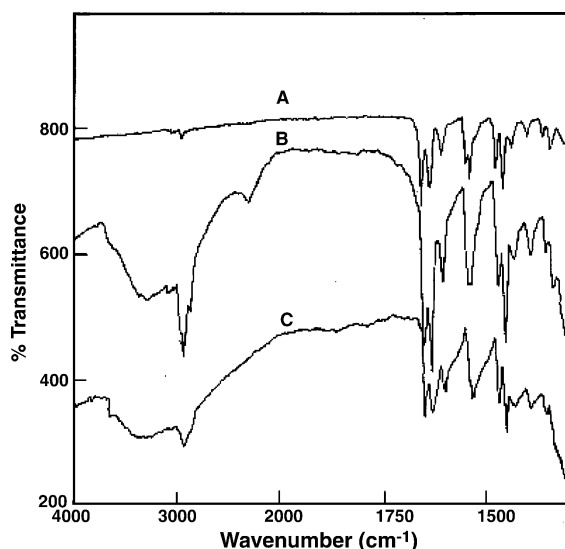
Fig. 1. FT-IR spectra of (A) Cu(salen), (B) Cu–S–AM(PS), (C) Cu(salen)–hexylamine.

Fig. 2. UV–Vis spectra of (A) Cu(salen), (B) Cu–S–AM(PS), (C) Cu(salen)–hexylamine.

complex. Therefore, the broad band at 3300 cm^{-1} is assigned to $>NH_2^+$ stretching, confirming the axial coordination between the amino group and the metal. This supports and gives direct evidence of immobilization of the complex through coordinate bonding as reported earlier by Zhou et al. [15]. Also, their observation that metal–salen complexes can not get immobilized on the walls of MCM-41 by mere adhesion is supported by the failure in immobilization of copper and cobalt salen complexes on HSi–MCM-41 in the present work. The bands in the region 1670–1300 cm^{-1} observed in the spectra of the complex containing samples are ascribed to C–C, C–O stretching modes in quasi-aromatic chelates in metal salens. The invariance in frequencies of Cu(salen) is due to as the coordinate bond being at right angles to the plane of the complex not affecting the structure of the complex in any significant manner. The adduct formation of cobalt salen with the amino group was also inferred from the similar nature of Co–S–AM(PS) spectrum (figure not shown).

3.4. Electronic spectroscopy

The UV–Vis electronic spectra of Cu(salen), Cu–S–AM(PS) and Cu(salen)–hexylamine adduct were recorded using nujol mull (Fig. 2). The UV–Vis electronic spectra of the salen ligand show typical absorptions at ∼253 and ∼326 nm attributable to ligand n–π* and π–π* charge transfer bands. Cu(salen) exhibits a broad band centered around ∼414 nm ascribed to ligand-to-metal charge transfer band similar to related metal (salen) compounds described in the literature [16,17]. After immobilization, the sample Cu–S–AM(PS) shows a narrow band centered at 368 nm overlapping the broad
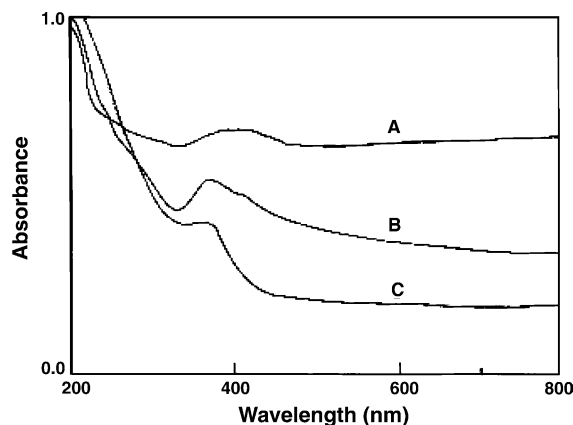
band at 326 nm. The adduct of Cu(salen)–hexylamine shows the band at 386 nm. By comparison of the spectra, it may be concluded that the occurrence of bands at 368 and 386 nm in the spectra of Cu–S–AM(PS) and Cu(salen)–hexylamine, respectively, is associated with axial lone pair coordination to the metal. Zangina et al. [18] have assigned the band at 375 and 421 nm to charge transfer from axial ligand to macrocycle and charge transfer from metal to axial ligand, respectively, in the spectra of iron(II) phthalocyanine complexes with phosphine or phosphite.

Thus the results obtained from IR and UV–Vis spectra are complementary indicating immobilization of Cu/Co complexes through coordinate bond between apical nitrogen and the metal.

3.5. EPR spectroscopy

EPR spectra of neat and immobilized Cu(salen) and Co(salen) complexes were recorded at 298 and 77 K. The spectra were typical of axial symmetry with $g_{II} = 2.183$ and $g_{\perp} = 2.084$. Hyperfine features due to Cu were not resolved due to intermolecular interactions. Single crystal X-ray structure of Cu(salen) revealed that the complex molecules form dimers with Cu–Cu separation of about 3.45 Å. This molecular association was reported to lead to the broadening of the EPR signals and the absence of metal hyperfine features [19]. The spectrum of the immobilized complex is similar to that of the neat complex. This similarity might arise from the oxygen–metal interaction observed in the dimer and the nitrogen lone pair coordination with the metal as well as the retention of planarity in the immobilized complex. When the complexes are heterogenized by encapsulation in Zeolite-Y, molecular isolation along with molecular distortion was observed. Metal hyperfine features were resolved and the spectrum was similar to that of frozen solutions. However, such a resolution is not observed in

Table 1
Physico-chemical properties of samples

Sample	S_{BET} (m²/g)	Pore volume (ml/g)	Pore diameter (Å)
HSi–MCM-41	1115	0.65	38.0
NH₂–MCM-41	569.0	0.34	26.0
Cu–S–AM(PS)	373.0	0.21	17.0
Co–S–AM(PS)	380.0	0.23	18.0
Cu–S–ASiO₂	169.0	–	–
Co–S–ASiO₂	254.0	–	–

Table 2
Thermal stability data

Sample	T^f (°C)	
	Loss expected (%)[a]	Loss observed (%)
HSi–MCM-41	10.2	18.4
Cu(salen)	76.0	76.5
Cu–S–AM(PS)	16.0	30.3
Co(salen)	77.0	74.3
Co–S–AM(PS)	17.0	29.8

T^f, final decomposition temperature.
[a] The values are calculated on the basic of estimated Cu (4%) and Co content (4.4%) in M–S–AM(PS).

the immobilized complexes studied in this work. These observations confirm that immobilization of MCM-41 does not result in the distortion of the salen complex as

pore dimensions are wide enough to accommodate the complex molecule. Co(salen) complexes did not exhibit ESR spectra due to short spin–lattice relaxation times.

3.6. Adsorption studies

The surface area, pore volume and pore diameters of as-synthesized, calcined and modified samples are given in Table 1. The decrease in mesopore volume (0.65–0.23 ml/g) and the surface area (1115–380 m²/g) are indicative of the grafting of the complex in the channels of HSi–MCM-41.

3.7. Thermal analysis

TGA (in air) profiles showed the decomposition of and Cu and Co salen complexes with residues amounting to cupric and cobaltous oxides, respectively (Table 2). The decomposition is complete at 516 and 460 °C for Cu and Co salen, respectively. However, on immobilization, the final decomposition temperatures are shifted to 651 and 572 °C for Cu(salen) and Co(salen), respectively. The increase observed for immobilized samples may be due to mutual stabilization of coordinating propylamino group and the complexes. The discrepancies observed in the experimental and expected results (Table 2) may be due to different amounts of adsorbed water present in the samples.

Table 3
Olefin oxidation using metal–salen catalysts and TBHP as oxidant (12 h data)

Catalyst	Amount (g)	Substrate	Conversion (mol%)	Product distribution (mol%)			TON
				EPO[a]	ONE[b]	Others	
Cu(salen)	0.02	Styrene	30.7	20.5	1.1	9.1	25
		Cyclohexene	29.7	1.4	21.5	6.8	24.8
		1-Decene	15.7	9.5	4.1	2.1	13.0
Cu–S[c]–AMSiO₂	0.05	Styrene	36.2	28.8	2.9	10.9	30.0
		Cyclohexene	32.4	1.3	22.4	8.7	26.8
		1-Decene	22.5	12.1	8.2	2.2	18.6
Cu–S[c]–AM(PS)	0.05	Styrene	68.5	52.5	1.8	14.2	56.8
		Cyclohexene	57.4	2.9	42.9	8.58	47.6
		1-Decene	38.8	22.2	12.4	3.4	32.2
Co(salen)	0.02	Styrene	40.4	26.2	2.1	12.1	33.0
		Cyclohexene	38.4	1.8	29.8	6.8	32.0
		1-Decene	19.5	11.3	6.1	2.1	16.2
Co–S[c]–AMSiO₂	0.05	Styrene	48.4	33.8	1.5	13.1	40.3
		Cyclohexene	38.4	2.3	26.4	9.7	32.0
		1-Decene	24.8	13.1	9.2	2.5	20.6
Co–S[c]–AM(PS)	0.05	Styrene	76.3	57.6	2.2	16.5	63.3
		Cyclohexene	61.3	3.2	48.4	9.7	50.0
		1-Decene	46.8	27.2	15.2	4.4	39.0

Conditions: Olefins 5 mmol, TBHP 5 mmol, acetonitrile 10 g, temp. 323 K.
[a] Epoxide.
[b] Ketone.
[c] Salen.

3.8. Catalytic reactions

The catalytic data for the epoxidation of styrene, cyclohexene and 1-decene are presented in the Table 3. It is observed that M–S–AM(PS) shows a higher conversion compared to the neat complex and M–S–AM-SiO$_2$ (where M = Cu and Co) Figs. 3(a) and (b). This is due to the increased adsorption of olefins on the hydrophobic surface of MCM-41. It is also noticed that the conversion rate decreases after 8 h for the neat complex and M–S–AMSiO$_2$, while the conversion pro-

ceeds to near completion on the immobilized catalyst with time. Also, as expected, styrene conversion is higher compared to the other olefins, Figs. 3(c) and (d). Further, in the oxidation of cyclohexene, the allylic hydrogen is more reactive than the C=C double bond towards the *t*-butyl peroxy radical and the reaction mainly gives the allylic oxidation product i.e. cyclohexenone [20], whereas in the case of styrene, the *t*-butyl peroxy radical attacks the double bond to give the epoxide. In the case of 1-decene, the allylic hydrogen is not that predominantly active. So both the products i.e.
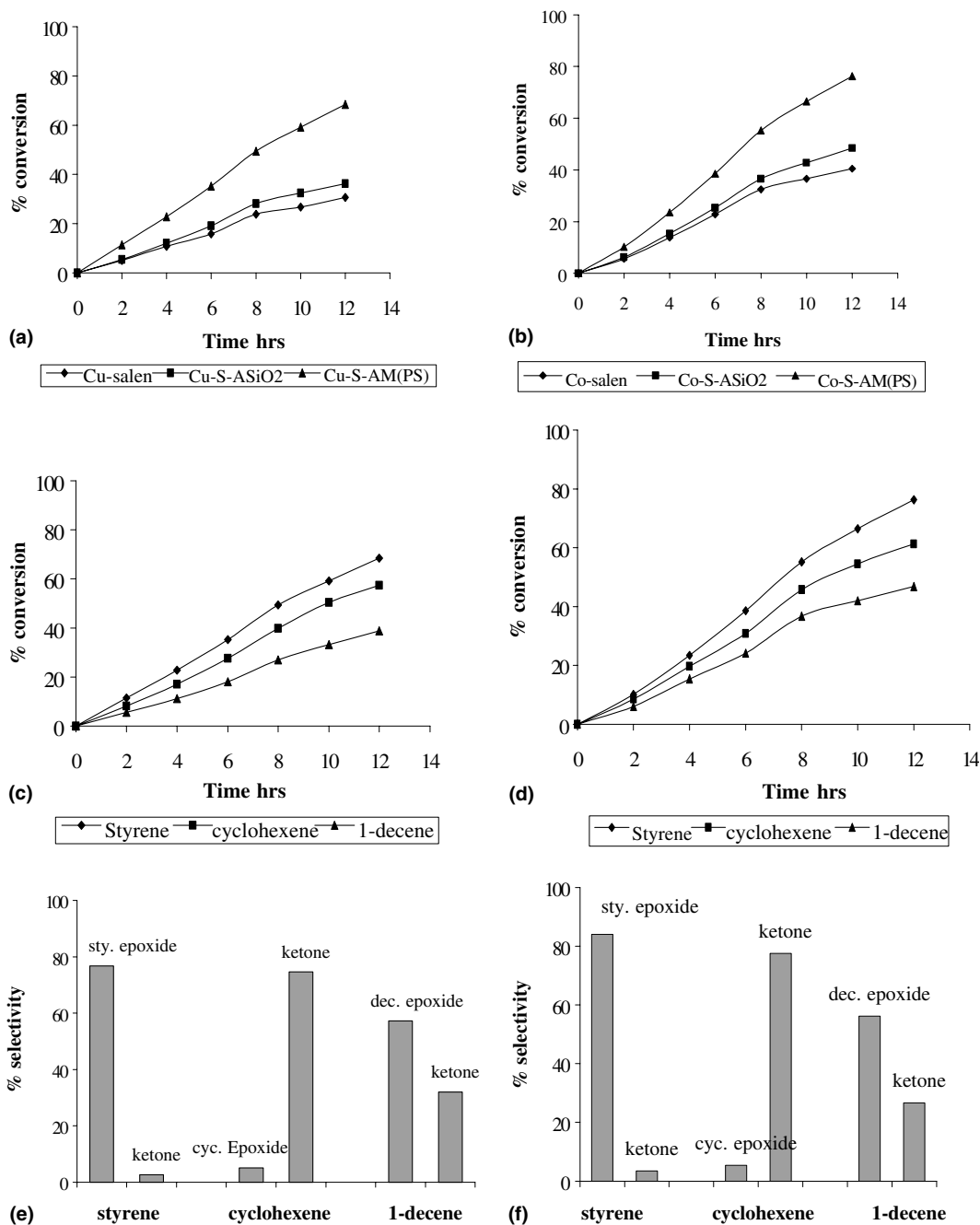

Fig. 3. (a) and (b) Styrene epoxidation on different catalysts of Cu–S–salen and Co–salen, respectively. (c) and (d) Olefin oxidation using Cu–S–AM(PS) and Co–S–AM(PS), respectively. (e) and (f) % Selectivity for Cu–S–AM(PS) and Co–S–AM(PS), respectively, for olefin oxidation.

epoxide and decenone are mainly observed, Figs. 3(e) and (f). Different reaction mechanisms have been proposed for the epoxidation of alkenes with peroxide [21,22]. The exact mechanism appears to depend on the reaction condition, the metal, the ligand and the substrate. The exact mechanism in the above reaction is not clear (Table 3).

4. Conclusions

The immobilization of Cu and Co (salen) complexes in the channels of HSi–MCM-41 molecular sieves with the walls modified by 3-APTES has been achieved by a post-synthesis method. Different characterization techniques such as XRD, FT-IR, EPR, UV–Vis and TG reveal that the complex is monomolecularly attached to the walls of MCM-41. NMR, FT-IR and UV–Vis spectra show the modification of the walls of MCM-41 with propylamine group. FT-IR and UV–Vis spectra show evidence for adduct formation of the amino group through the axial coordination with the metal which enhances the catalytic activity. The molecular dispersion of the complex with sufficient void space and the hydrophobic surface are appropriate for activation of hydrocarbons as evidenced by higher TON's on immobilization.

Acknowledgements

References

[1] T. Mallat, A. Baikar, Catal. Today (2000) 57.

[2] J.T. Groves, R.C. Haushalter, M. Nakamura, T.E. Nimo, B.J. Evans, J. Am. Chem. Soc. 103 (1981) 2884;
R.H. Felton, G.S. Owens, D. Dolphin, J. Fajer, J. Am. Chem. Soc. 93 (1971) 6332.

[3] R.H. Holm, Chem. Rev. 87 (1987) 1401.

[4] P.S. Dixit, K. Shrinivasan, Inorg. Chem. 27 (1988) 4507.

[5] F. Lloret, M. Julve, M. Mollar, I. Castro, J. Latorre, J. Faus, X. Solans, I. Morgenstern-Badaran, J. Chem. Soc., Dalton Trans. (1989) 729.

[6] B.M. Camine, S.R. Doctrow, PCT Int. W09640148AAI, 1996.

[7] D.E. De Vos, P. Knops-Gerrits, R.F. Parton, B.M. Weckhuysen, P.A. Jacobs, R.A. Schoonheydt, J. Ind. Phenom. Mol. Recog. Chem. 21 (1995) 185.

[8] P.P. Paul, Prog. Inorg. Chem. 48 (1999) 457.

[9] K. Balkus Jr., M. Eissa, R. Levedo, J. Am. Chem. Soc. 117 (1995) 10753.

[10] C.T. Kresge, M.E. Leonowicz, W.J. Roth, J.C. Vartuli, US Patent 5 098 684, Mobil Oil Corporation, 1992.

[11] C.T. Kresge, M.E. Leonowicz, W.J. Roth, J.C. Vartuli, J.S. Beck, Nature 359 (1992) 710.

[12] A. Bottcher, H. Elian, E.-G. Jager, H. Langfelderova, M. Mazur, L. Muller, H. Paulus, P. Pelikan, M. Rudolph, M. Valko, Inorg. Chem. 32 (1993) 4131.

[13] P. Karandikar, M. Agashe, K. Vijaymohanan, A.J. Chandwadkar, Appl. Catal. A (accepted).

[14] A.B. Sorokin, A. Tuel, Catal. Today 57 (2000) 45.

[15] X.-G. Zhou, X.-Q. Yu, J.-S. Huang, S.-G. Li, L.-S. Li, C.-M. Che, Chem. Commun. (1999) 1789.

[16] I.E. Kingma, M. Wiersma, J.L. Van der Baan, S. Balt, F. Bickelheanpt, M.W.G. de Bolster, G.W. Klumpp, A.L. Spek, J. Chem. Soc., Chem. Commun. (1993) 832.

[17] A. Bigotto, E. Reisenhofer, R. Giordani, Spectrochem. Acta A 40 (1984) 203.

[18] A. Zangina, M. Byo-Bangoura, K. Bayo, G.V. Quedrago, Bull. Chem. Soc. Ethiopia 16 (1) (2002) 73.

[19] S. Seelan, A.K. Sinha, D. Srinivas, S. Sivasanker, J. Mol. Catal. A 157 (2000) 163.

[20] Z.-R. Lu, Y.-Q. Yin, D.-S. Jin, J. Mol. Catal. 70 (1991) 391.

[21] M.R. Cramarossa, L. Forti, M.A. Fedotov, L.G. Detusheva, V.A. Likholobov, L.I. Kuznetsova, G.L. Semin, F. Cavani, F. Trifiro, J. Mol. Catal. A 127 (1997) 85.

[22] N. Komiya, T. Naota, Y. Oda, S. Murahashi, J. Mol. Catal. A 117 (1997) 21.